International Journal of Recent Technology and Engineering (IJRTE)
ISSN: 2277-3878, Volume-8 Issue-3, September 2019

Numerical Simulation of Flow over a Flat Unglazed Transpired Solar Collector (UTC) and it's Performance Prediction

Sp Panigrahi, S K Maharana

Abstract: ***An unglazed transpired solar collector is a system that can leverage the abundant solar energy for various purposes. The solar collector is available in flat or corrugated form and is seen to be installed as an exterior layer of building facades. The cladding thus made absorbs radiation from the sun and heats up air being sucked by fan and flowing through perforations. In this research the focus has been to understand the correlation of plate temperature, exit temperature, the velocity distribution in the chamber and perforation location when air flows past an unglazed transpired solar collector (UTC). The establishment of correlations was carried out in the dataset of flow variables obtained after solving the problem using Navier-Stokes (NS) equations along with standard two-equation (k-ε) turbulence models and Shear Stress Transport (SST) k-ω models for turbulent flow. The same problem was also solved using NS equation using laminar model. An attempt has also been made to compute Pearson's correlation coefficient of any two variables to understand their strong and weak correlations. A linear regression analysis was done through an open source software Rstudio for a dataset produced during the computational modeling using a commercial CFD solver, Ansys® Fluent. At the end a Monte Carlo simulation has been done to predict the likelihood of using the flat UTC for drying as well as to understand the dependency of system efficiency on plate exit temperature, suction velocity and freestream temperature.***

Keywords Unglazed Transpired Solar Collector (UTC), turbulent models, Suction velocity, Exit temperature,

I. INTRODUCTION

Unglazed transpired solar collectors (UTC's) are now a well-recognized solar air heater for heating outside air directly. They are key components in many engineering applications, such as in institutional and residential heating, industrial processes like sewage wastewater treatment, and food processing [Siwei Li et al., 2014]. The solar collector is available in flat or corrugated form and is seen to be installed as an exterior layer of building facades.

Manuscript published on 30 September 2019
* Correspondence Author
Sp Panigrahi*, Mechanical Engineering, Faculty Of Engineering, Christ(Deemed To Be University), Bangalore, India. Email: Sajna.Panigrahi@Gmail.Com
Sk Maharana, Aeronautical Engineering, Acharya Institute Of Technology, Bangalore, India. Email: Skmaha123@Gmail.Com

The cladding thus made absorbs radiation from the sun and those heats up air being sucked by fan and flowing through perforations. The hot air is usually collected at the outlet for preheating of ventilation air, for producing hot water and for cooling using desiccants in domestic environment (Athienitis et al., 2011).

Out of two forms of UTC such as flat and corrugated, the corrugated form of UTC has reported to have 70% higher efficiency (Bambara, 2012) than the flat one when both are integrated with photovoltaic systems for the generation of electricity and heat. Typically, the flow of air over the UTCs is driven by mechanical fans. The solar radiation that falls on the UTC creates thermal buoyancy effect and the formation of atmospheric boundary layer is observed to be developed on UTC. Both the buoyancy effect and boundary layer on UTC complicates the other important phenomena such as impingement, separation, reattachment that are expected to happen on the perforated UTC. The airflow over and through the perforations of UTC plate has different Reynolds number. It is in the order of 10^3 (laminar flow) when the flow is through perforation and 10^6 (turbulent flow) while the airflow is over the plate. This confirms that there is a transition of flow happening between laminar to turbulent states. The local flow situation gets even more complex due to the presence of low porosity of plate (0.5–2 %) is attributed to the small perforation. The flow transition and small perforation contribute towards a non-homogeneity of suction of flow through perforation. However there exits classical research findings on homogeneous suction by early outstanding researchers [Iglisch (1944), Kay (1948), Schlichting and Gersten (2000)]. In their studies perforation spacing of a few millimeters was used and the vertical velocity at the plate surface was assumed which led to the availability of an asymptotic solution of velocity field. So, a difference between the types of suction (homogeneous and non-homogeneous) of flow over plate is found in the earlier studies over UTC.

In this research the focus has been to understand the correlation of plate temperature, exit temperature and the velocity distribution in the chamber when air flow past an unglazed transpired solar collector (UTC) by using the using Navier-Stokes (NS) equations along with standard two-equation (k-ε) models and Shear Stress Transport (SST) k-ω models for turbulent flow.

Monte Carlo simulation has been done to predict the likelihood of using the flat UTC for drying as well as to understand the dependency of system efficiency on plate exit temperature, suction velocity and free stream temperature.

II. GOVERNING EQUATIONS OF FLOW

The conservation forms of three governing equations are given below. Each of these equations is time-averaged and presented below: Mass conservation equation:

$$\frac{\partial \rho}{\partial t} + \frac{\partial \rho u_i}{\partial x_i} \qquad (1)$$

Momentum conservation equation:

$$\frac{\partial \rho u_i}{\partial t} + \frac{\partial (\rho u_i u_j + p\delta_{ij})}{\partial x_j} = \frac{\partial (\tau_{ij} - \rho \overline{u_i u_j})}{\partial x_j} \qquad (2)$$

Energy conservation equation:

$$\frac{\partial (\rho \varepsilon_o)}{\partial t} + \frac{\partial (\rho \varepsilon_o u_i + p u_i)}{\partial x_i} = \frac{\partial (\tau_{ij} u_j - \rho \overline{u_i u_j} u_j)}{\partial x_i} - \frac{\partial (q_i + C_p \rho \overline{u_i \vartheta})}{\partial x_i} + \frac{\partial}{\partial x_i}\left[\left(\mu_l + \frac{\mu_t}{\sigma_k}\right)\frac{\partial k}{\partial x_i}\right] \qquad (3)$$

Turbulence Models: One of the turbulence models used in this research is k-ε. The description of which is outlined below.

The two-equation (k-ε) turbulence models, given below, have been used in the Reynolds Averaged Navier-Stokes (RANS) equations only to model the turbulent quantities.

$$\frac{\partial \rho k}{\partial t} + \frac{\partial \rho u_j k}{\partial x_j} = -\rho \overline{u_j u_i}\frac{\partial u_i}{\partial x_j} + \frac{\partial}{\partial x_j}\left[\left(\mu_l + \frac{C_\mu k^2}{\overline{\sigma_k} \varepsilon}\right)\frac{\partial k}{\partial x_j}\right] - \rho\varepsilon(1 + M_\tau^2) \qquad (4)$$

$$\frac{\partial \rho \varepsilon}{\partial t} + \frac{\partial \rho u_j \varepsilon}{\partial x_j} = -C_{\varepsilon 1}\rho \overline{u_j u_i}\frac{\partial u_i}{\partial x_j}\frac{\varepsilon}{k} + \frac{\partial}{\partial x_j}\left[\left(\mu_l + \frac{C_\mu k^2}{\overline{\sigma_k} \varepsilon}\right)\frac{\partial \varepsilon}{\partial x_j}\right] - f_2 \rho \overline{C_{\varepsilon 2}}\frac{\varepsilon}{k}\left[\varepsilon - v_l\left(\frac{\partial \sqrt{k}}{\partial n}\right)^2\right] \qquad (5)$$

Where

$C_\mu = 0.09$, $C_{\varepsilon 1} = 1.44$, $\overline{\sigma_k} = \sigma_k = 1.4$, $\overline{\sigma_\varepsilon} = \sigma_\varepsilon = 1$ and $\overline{C_{\varepsilon 2}} = C_{\varepsilon 2} = 1.92$, $f_\mu = \exp\left[\frac{-3.41}{\left(1 + \frac{R_T}{50}\right)^2}\right]$; $R_T = \frac{k^2}{\mu_t \varepsilon}$; $f_2 = 1 - 0.3\exp(R_T^2)$

Boundary conditions for epsilon (ε) and k at the wall are

$$\varepsilon_{wall} = v_l\left(\frac{\partial \sqrt{k}}{\partial n}\right)^2; \; k_{wall} = 0$$

The turbulent stress components are

$$\rho \overline{u_j u_i} = 2\rho v_t S_{ji} - \frac{2}{3}\delta_{ji}\rho k \quad \text{and} \quad S_{ji} = \frac{1}{2}\left[\frac{\partial u_j}{\partial x_i} + \frac{\partial u_i}{\partial x_j}\right] - \frac{1}{3}\delta_{ji}\frac{\partial u_j}{\partial x_i}$$

III. METHODOLOGY

The geometry, flow domain and different surfaces used for boundary conditions chosen for the simulation study are shown in Fig.1 (a). The UTC plate used in the study has an area of 0.6 m x 0.6 m and the cavity has a height of 0.15 m. Each perforation diameter is 0.00159 m and the pitch (distance between two perforations) is 0.01689 m. The thickness of wall is 0.00086 m .The upper part of the domain from the cavity surface is 0.3 m. This is sufficient enough to accommodate the growth of boundary layer. The boundary conditions are defined below in the Table 1 and the same has been depicted in a schematic diagram for the flow domain in X-Y plane in Fig.2.

TABLE 1: Boundary Conditions

Surface Number	Boundary condition type	Flow variable
1	Inlet	Free stream velocity is 1 m/s and temperature is 298 K and Turbulent Intensity is chosen as 1 %
2	Wall	Heat flux (solar radiation) is 600 Watt/ m^2
3	Outlet	Gauge pressure is equal to zero
4	Wall	Adiabatic wall (heat transfer across the wall, Q=0)

The computations of the flow variables were carried out using the established SIMPLE algorithm. It is to be noted that the flow velocity at the approach(surface 1) varies between 0 to 1 m/s and the value of the suction velocity at the plate exit (surface 2) varies from 0.045 to 0.077 m/s. These were verified during experiments as well.

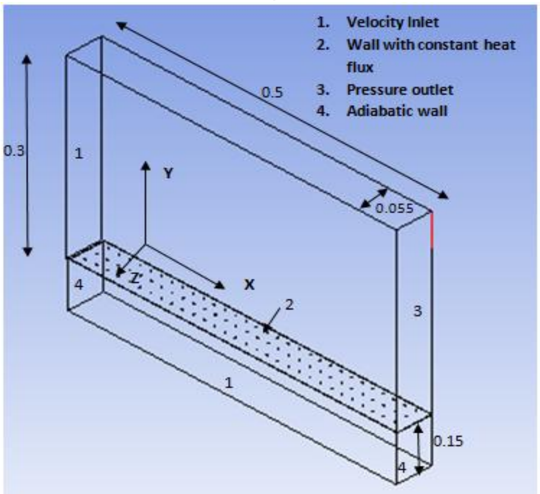

Fig. 1(a) Flat UTC model configuration (unit: m) – Computational Domain

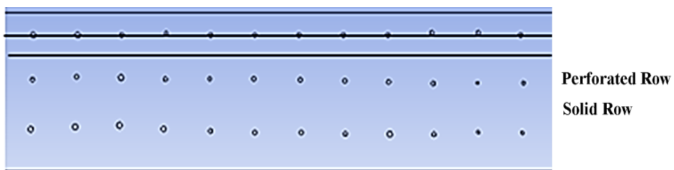

Fig. 1(b) Sketch of perforated and solid rows

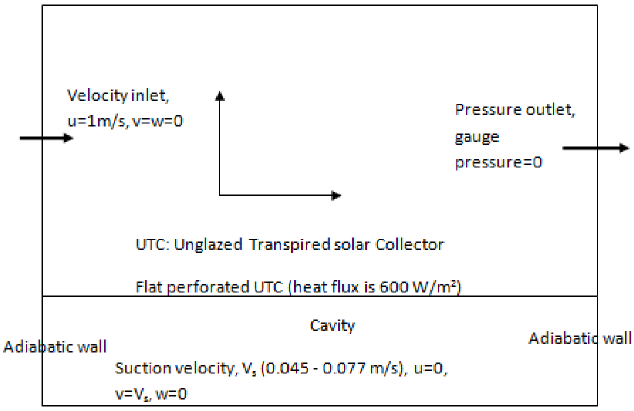

Fig. 2 Schematic diagrams with boundary condition for the flow domain in X-Y plane

Convergence and Mesh Independence Test

The residuals were intermittently calculated by the solver and an absolute value of tolerance of 10^{-6} was chosen for all variables to meet for their convergence. A grid independence test was carried out to verify if the acceptance of the value of each variable computed three different grid resolutions of the domain does not change and the summary of the study is presented in Table 2.

Table 2 Grid Independence Test

Plate Temperature / Cavity Outlet Temperature [K]	Cell Numbers			Experimental Data
	Grid 1 (286000)	Grid2 (200000)	Grid3 (135000)	
Case 1:	314.0/305.9	314.5/305.7	314.7/305.0	313.9/306.5
Case 2:	315.4/307.	314.8/307.1	313.7/306.9	313.9/306.5

Case 1: wind speed=1m/s and suction velocity=0.077m/s
Case 2: wind speed=1m/s and suction velocity=0.045m/s

IV. RESULTS AND DISCUSSION

The cases presented only in Table 3 are the ones which were considered for validation between simulation and experimentation. The Fig. 3 shows a comparison of (a) plate temperature and (b) cavity exit temperature computed from CFD solver with those obtained from experiments. The matching between the numerical results and their validation is quite good and hence acceptable. The simulated results using two-equation (k-ε) turbulence closure model were more consistent and stable in terms of convergence as compared to those obtained from the standard shear stress k-ω model. However, all the models predict identical results when the cavity temperature was noted.

Table 3 Tested cases for model validation

Cases	1	2
Freestream wind speed[m/s]	1	1
Suction velocity [m/s]	.045	.077

The laminar and SST k-ω are also considered for comparison and presented below.

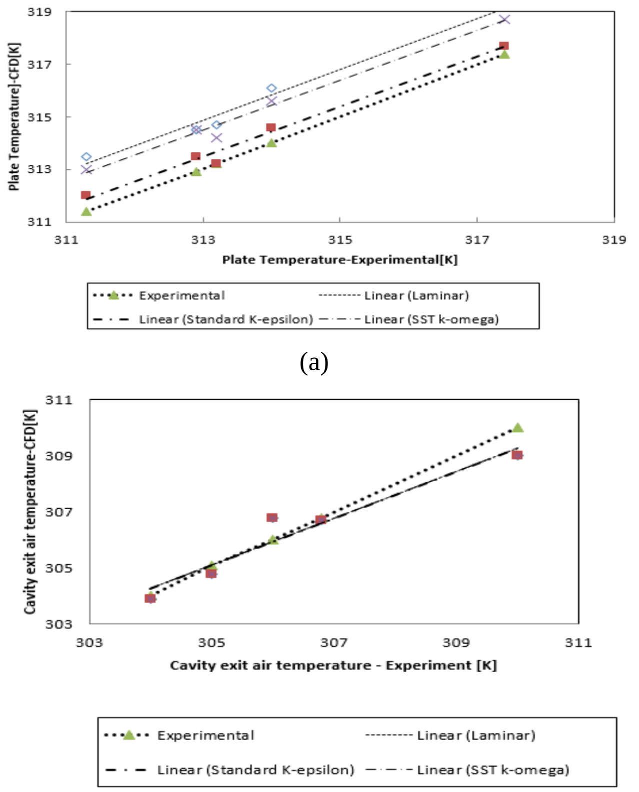

(a)

(b)

Fig. 3 Validation of results for flat UTC model: (a) plate temperature [in K] and (b) cavity exit air temperature[in K].

From the Fig.4 it is observed that the mean y-component of velocity predicted by k-ε turbulence model is more chaotic in the cavity zone compared to that predicted by k-ω turbulence model. The velocity variation is predictable and follows a pattern in case of k-ω. TheFig. 5 shows a comparison of velocity profile, U_y of air within the chamber predicted by 3 different models k-ω , laminar and k-ε for suction velocity, V_s= 0.077 m/s. Although the variations by all the three models look similar, at Y=0.011, the higher value of U_y is predicted by the Laminar model. It supersedes k-ε and k-ωwhich predicts the lowest value. Between Y=0.21 and 0.31 (middle of the cavity) the U_y predicted by all models rises sharply and remains almost the same. From Y=0.31 to 0.51, the U_y rises. This change of variation is due to the inherent nature of the flow near the walls (velocity component is towards lowest value) friction deters the growth of velocity and near the surface of UTC (perforated one) the speed is hugely affected by the suction velocity and it adds to increase the magnitude of U_y.

The temperatures predicted [shown in Fig.6] by laminar model are higher than that predicted by other two turbulence models in the region indicated by Y=0.31 to 0.5. For the suction velocity V_s=0.077 m/s, the cavity exit air temperature is rising from 298 K to 318.2 K. For suction velocity Vs=0.045 m/s, the plate temperatures predicted by all three models start rising from 302 K. The highest value of the temperature predicted by the laminar model is 348 K.

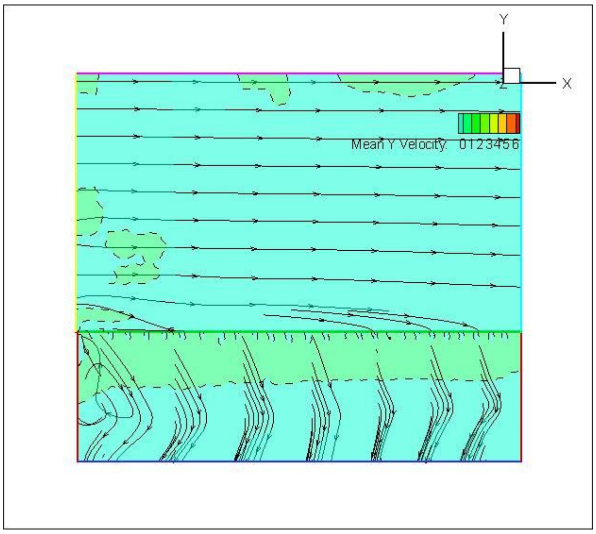

Fig. 4 Mean U_y velocity and pathlines in the cavity predicted by CFD [k-ω]

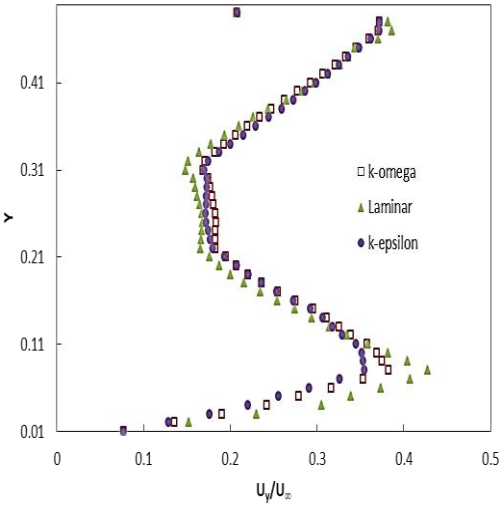

Fig. 5 Comparison of velocity profile, U_y of hot air within the chamber predicted by 3 different models k-ω , Laminar and k-ε for suction velocity, V_s= 0.077 m/s

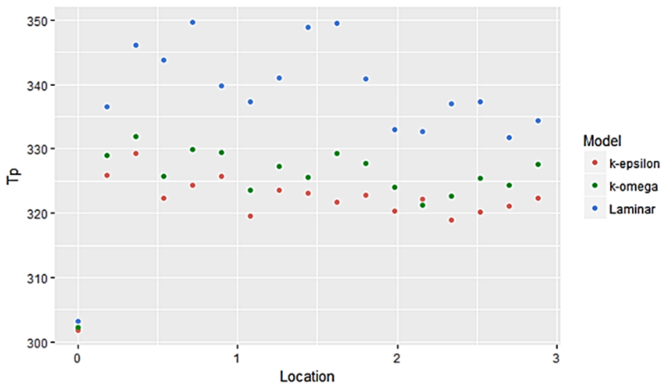

Fig. 6 Comparison of Plate Temperatures predicted by 3 different models k-ω (k-omega), Laminar and k-ε (k-epsilon) for suction velocity, Vs= 0.077 m/s

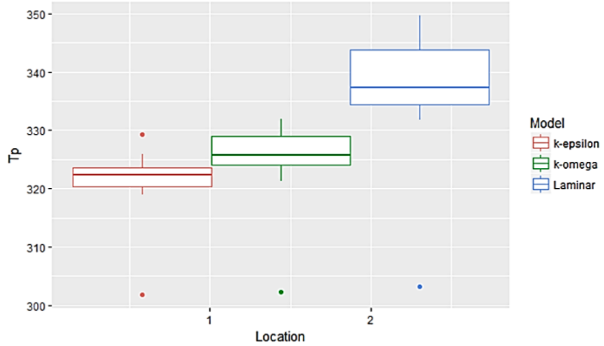

Fig. 7 Box plots to show the range and characteristics of plate temperatures predicted by 3 different models k-ω (k-omega), laminar and k-ε (k-epsilon) for suction velocity, V_s= 0.077 m/s

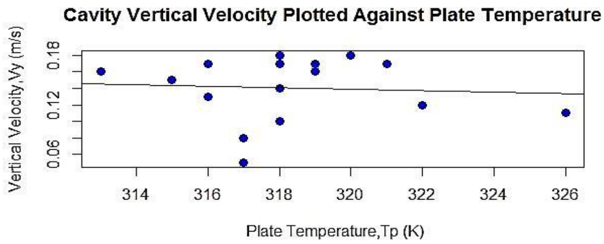

Fig. 8 Cavity vertical velocity versus plate temperature with regression line

Fig.8 shows cavity(or chamber) vertical velocity versus plate temperature variation where a regression line is passing through the variation and it is noted that there is a slightly increasing linear relationship between plate temperature and vertical velocity. The variation around the estimated regression line is not constant but an assumption of equal error variance is reasonable in this case.

Table 4 shows correlation among perforation location in flat UTC, numerical plate temperature(Tp), vertical velocity(Vy), exit temperature(Te),experimental plate temperature(Tpe) and experimental exit temperature(Tee). It shows a measure of the direction and strength of the relationship between two variables. It is measured by the Pearson's correlation coefficient(r) that varies between -1 and +1. Correlation does not mean causation. A strong relationship between any two variable does not necessarily mean that one causes the other. From the table it's noted that location has strong correlation with cavity vertical velocity and weaker correlation exit temperature and plate temperature.

TABLE 4: Correlation Matrix

	Location	Tp	Vy	Te	Tpe	Tee
Location	1.0000000	0.29128708	-0.84019410	-0.11855473	0.32527117	-0.15992938
Tp	0.2912871	1.00000000	-0.06836903	0.04134775	0.98613232	0.06276044
Vy	-0.8401941	-0.06836903	1.00000000	0.34769628	-0.11256077	0.37392206
Te	-0.1185547	0.04134775	0.34769628	1.00000000	0.02441527	0.99563585
Tpe	0.3252712	0.98613232	-0.11256077	0.02441527	1.00000000	0.04508812
Tee	-0.1599294	0.06276044	0.37392206	0.99563585	0.04508812	1.00000000

Monte Carlo simulation has been used to model the probability of different outcomes in a process that cannot easily be predicted due to the intervention of random variables. It is a technique used to understand the impact of risk and uncertainty in prediction and forecasting models.

In this research system thermal efficiency (η)[6]was computed. That is given as ρ x V_s x C_p x (Te-T_∞)/G, where density of air (ρ) is 1.22 kg/m^3, suction velocity is kept between .045 m/s and 0.077 m/s, specific heat capacity of air at constant pressure(C_p) is 1.005 KJ/KgK, exit temperature (Te) and freestream temperature(T_∞) are in kelvin(K) and solar radiation(G) on UTC is in Watt/m^2. The simulation was run for 1000 times to compute the likelihood (41%) of efficiency that could be acceptable for use. The acceptability of use was decided based upon the drying capacity of UTC . The simulation also predicted the likelihood of $T_e$going greater than 325 K (close to 52 ^{o}C) where drying is possible and it affects the system efficiency. From the Fig.9 it is also noted that the likelihood of freestream (T_∞) affecting the system efficiency is about 54% in this study. Similarly the chamber where the heat is collected could be used for drying (typical range of drying is 10^{o}C to 15^{o}C) purpose. The suction velocity affects the efficiency. From the simulation it is observed that the likelihood is 52% for V_s which is greater than 0.06 m/s that would affect efficiency.

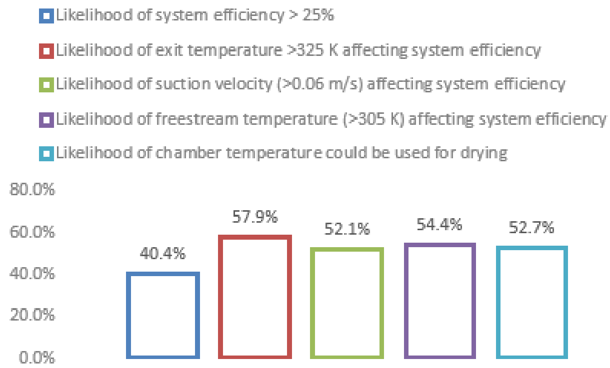

Fig.9 Likelihood of different variables affecting system efficiency

V. CONCLUSIONS

The numerical simulation of fluid flow and heat transfer through a perforated flat UTC was carried out. In this research the focus has been to understand the correlation of plate temperature, exit temperature and the velocity distribution in the chamber when air flow past an unglazed transpired solar collector (UTC) and predict the performance of the system using computational method. An attempt has also been made to compute Pearson's correlation coefficient of any two variables to understand their strong and weak correlation. The regression analysis and Pearson's correlation coefficient values have strengthened the fact that there is a strong correlation between cavity vertical velocity, perforation location and temperature. The Monte Carlo simulation predicted the likelihood of $T_e$going greater than 325 K (close to 52 ^{o}C) and in this case drying by hot air collected in the cavity(or chamber) is possible and it also affects the system efficiency. The simulation also revealed that the likelihood of system efficiency getting affected by key decision variables such as suction velocity(V_s), plate exit temperature(T_e) and freestream temperature(T_∞).

REFERENCES

1. C. V. Croitoru, I. Nastase, F. I. Bode and A. Meslem, "Thermodynamic investigation on an innovative unglazed transpired solar collector", Solar Energy 131, pp. 21–29 (2016).
2. Roozbeh Vaziri, M. Ilkan, F. Egelioglu, " Experimental performance of perforated glazed solar air heaters and unglazed transpired solar air heater", Elsevier, Solar Energy Volume Solar Energy 119 pp. 251–260 (2015)
3. Siwei Li, Panagiota Karava, Sam Currie, William E. Lin and Eric Savory, "Energy modeling of photovoltaic thermal systems with corrugated unglazed transpired solar collectors" – Part 1: Model development and validation, ELSEVIER, Solar Energy 102, pp.282–296(2014)
4. Siwei Li, Panagiota Karava, Sam Currie, William E. Lin and Eric Savory, "Energy modeling of photovoltaic thermal systems with corrugated unglazed transpired solar collectors" – Part 2:Performance analysis, Elsevier ,Solar Energy 102**,** pp. 297–307(2014)
5. Michael R. Collins and Hani Abulkhair, An evaluation of heat transfer and effectiveness for unglazed transpired solar air heaters, Elsevier, Solar Energy 99**,** pp. 231–245 (2014)
6. Siwei Li, Panagiota Karava, Eric Savory, William E. Lin, "Airflow and thermal analysis of flat and corrugated unglazed transpired solar collectors", Elsevier, Solar Energy 91**,** pp.297-315(2013)
7. Messaoud Badache, Daniel R. Rousse , Stéphane Hallé, Guillermo Quesada and Guillermo Quesada, "Experimental and numerical simulation of a two-dimensional unglazed transpired solar air collector", ELSEVIER, Solar Energy 93**,** pp. 209–219 (2013)
8. Siwei Li and Panagiota Karava, "Evaluation of turbulence models for airflow and heat transfer prediction in BIPV/T systems optimization", Elsevier, Energy Procedia 30**,** pp. 1025 – 1034 (2012)
9. Arulanandam, S.J., Hollands, K.G.T. and Brundrett, E., "A CFD heat transfer analysis of the transpired solar collector under no-wind condition".Solar Energy 67, pp. 93–100 (1999)
10. Athienitis, A.K., Bambara, J., O'Neill, B., Faille, J., A prototype photovoltaic/thermal system integrated with transpired collector. Solar Energy 85, pp. 139–153(2011)
11. Gawlik, K.M., "A numerical and experimental investigation of heat transfer issues in the practical utilization of unglazed, transpired solar air heaters" Ph.D. Thesis(1993), Department of Civil, Environmental, and Architectural Engineering, University of Colorado, Colorado, USA.
12. Iglisch, R., 1944. Exact calculation of laminar boundary layer in longitudinal flow over a flat plate with homogeneous suction. Schriften der Deutschen Akademie der Luftfahrtforschung, Band 8B, Heft 1.Translation: NACA TM No. 1205

AUTHORS PROFILE

SP Panigrahi is currently an Asst. Professor in the Dept. of Mechanical Engineering, Faculty of Engineering, Christ (Deemed to be University), Bangalore. She has got 9 years of teaching and research experience . She received her MTech from VTU, Karnataka and BE from BPUT, Odisha.

Dr SK Maharana is currently professor and head of Aeronautical Engineering, Acharya Institute of Technology. He obtained his M.Tech and PhD degrees from the department of Aerospace Engineering, IIT Kharagpur. He is a life member of ISTE and ISWE. He has worked in one of the most admired aviation industries and has got 13 years of teaching experience with 35+ publications in different journals and conferences.